PHYSICAL REVIEW B, VOLUME 63, 100508(R)

Observations of a pseudogap in the *c*-axis electronic Raman continuum of $YBa_2Cu_4O_8$ single crystals

J. W. Quilty, S. Tajima, and S. Adachi
Superconductivity Research Laboratory, International Superconductivity Technology Center, 1-10-13 Shinonome, Koto-ku, Tokyo 135-0062, Japan

A. Yamanaka
Chitose Institute of Science and Technology, Chitose, Hokkaido 066-8655, Japan
(Received 28 August 2000; published 21 February 2001)

We report the results of *c*-axis polarized electronic Raman scattering measurements on single crystals of $YBa_2Cu_4O_8$. As the temperature is lowered we find a monotonic depletion of spectral weight below a Raman shift of around 900 cm^{-1}, consistent in character with the pseudogap, but unaffected by the onset of superconductivity. We also establish that the *c*-axis continuum in $YBa_2Cu_4O_8$ can be described by a simple relaxational response, without the inclusion of electron-phonon scattering effects. In contrast to the *c*-axis transport properties, the CuO chains appear to have little influence on the *c*-axis Raman continuum.

DOI: 10.1103/PhysRevB.63.100508 PACS number(s): 74.72.Bk, 74.25.Gz, 78.30.−j

The high-temperature superconducting cuprate (HTSC) materials exhibit features that have been persistent puzzles to the solid-state community since their discovery. One well-known conundrum is the suppression of electronic excitations in the normal state of underdoped superconductors, the ''pseudogap.''[1] The charge dynamics of these highly anisotropic systems have provided an equally enduring puzzle. In particular, the *c*-axis charge transport in $YBa_2Cu_4O_8$ (Y124), a stoichiometric and naturally underdoped member of the YBCO family, shows a curious crossover from incoherent to coherent transport with decreasing temperature.[2,3] Evidence of a pseudogap in Y124 has been obtained by nuclear magnetic resonance,[4,5] *c*-axis optical conductivity,[6] and *ab*-plane Raman spectroscopy,[7,8] amongst other techniques.

Meanwhile, the high-frequency *c*-axis electronic Raman continua of both Y124 and the related $YBa_2Cu_3O_{7-\delta}$ (Y123) are accurately described by a relaxational response[9–13] which might arise from either impurity or phonon scattering processes.[14–16] In the case of Y123 it has been proposed that scattering from the apical O(4) phonon mode gives rise to the continuum and contributes an incoherent term to the *c*-axis transport via phonon assisted interlayer hopping.[11–13] While Y123 and Y124 are closely related structurally, their *c*-axis transport properties differ markedly. Underdoped Y123 exhibits insulating *c*-axis resistivity as a function of temperature, while Y124 and stoichiometric Y123 display metallic resistivity. The CuO chains have been implicated as the source of the coherent *c*-axis transport in these materials.[2,17]

Despite this, the low-frequency electronic Raman continuum, in the vicinity of the strong phonon bands, has thus far not been the subject of detailed study in either Y124 or Y123. We were therefore interested in investigating the nature and temperature dependence of the low-frequency Y124 *c*-axis electronic Raman continuum, which has received relatively little attention.

Single crystals of Y124 were grown using a self-flux method described elsewhere,[18] producing crystals of typical dimensions $0.4\times0.2\times0.1$ mm^3 and 80 K T_c (onset) determined by magnetic susceptibility measurements. Our Raman spectrometer consisted of a Jobin-Yvon T64000 triple monochromator and charge coupled device. Exciting radiation was provided by the 514.5 nm line of an Ar-Kr laser, point focussed to a spot of approximate diameter 100 μm and incident power of 1 mW. Measurements of the Stokes to Anti-Stokes intensity ratio revealed no detectable sample heating and we quote nominal sample temperatures. The light was incident on the *bc* face of the crystals in pseudobackscattering geometry and *zz* polarization (*z* parallel to the crystallographic *c*-axis), selecting excitations of A_g symmetry. Spectra taken in *yz* polarization showed no significant continuum scattering. In all spectra shown, the Bose factor contribution has been removed and the intensity normalized in the region 1200–1300 $cm^{-1}$to correct for small alignment differences between measurements. We assume that the high-frequency electronic continuum exhibits negligible temperature dependence.

Typical *c*-axis spectra at temperatures of 300 and 100 K are shown in Fig. 1 for one crystal studied. Spectra from the other crystal discussed here were in excellent agreement as a function of temperature and Raman shift, confirming the absence of sample dependent effects. Six strong, asymmetric phonon lines dominate the *c*-axis Raman spectrum, obscuring both the frequency and temperature dependence of the underlying electronic continuum. Weak peaks in the vicinity of 1000 cm^{-1} are second-order phonon scattering processes.[19]

If the 300 and 100 K spectra are compared, a depletion of spectral weight extending to around 900 cm^{-1} may be observed. The origin of the depletion, however, is difficult to determine from the raw spectra due to the temperature de-

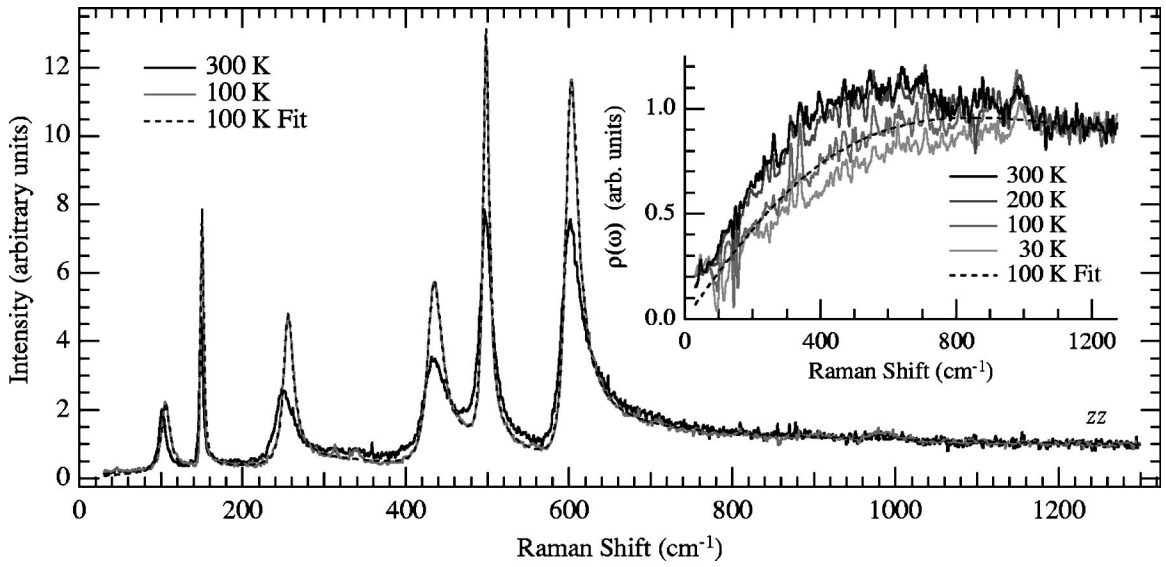

FIG. 1. *c*-axis polarized Raman spectra at temperatures of 300 and 100 K from a single crystal of Y124 ($Tc = 80$ K). The spectra have been corrected for the Bose factor contribution. A fit to the 100 K spectrum is shown by the dashed line. Note the anomalous depletion of the continuum observable between spectra. Inset: electronic Raman spectra at temperatures of 300, 200, 100, and 30 K with the phonon contribution subtracted via Eq. (1). The fit at 100 K is shown for comparison.

pendence of the phonon lineshapes. Separating a strongly interacting phonon contribution from the electronic continuum is a common problem in the analysis of HTSC Raman spectra, but the often-used Fano lineshape proved to be inadequate for analyzing our *c*-axis spectra.

We therefore considered the more complex Green's function description of the Raman intensity $I(\omega)$. This approach has been used previously,[20] and we extend the method by summing over the six observed phonon modes which are permitted to interact with the Raman active continuum thus:

$$I(\omega) = A[n(\omega)+1]\left(\rho(\omega) + \sum_{i=1}^{6} \frac{1}{\gamma_i(1+\epsilon_i^2)}[S_i'^2 + 2\rho(\omega)\epsilon_i V_i S_i' - V_i^2\rho(\omega)^2]\right), \quad (1)$$

where $\epsilon_i = (\omega - \omega_{\nu,i})/\gamma_i$ and $S_i' = (T_i' + V_i R(\omega))$. A is an overall intensity factor, $n(\omega)$ is the Bose-Einstein thermal factor (removed from our spectra by division), and $R(\omega)$ and $\rho(\omega)$ are the real and imaginary parts of the electronic response function $\chi(\omega)$. For each phonon *i*, T_i' is the ratio of the transition matrix elements for phononic and electronic excitations, V_i is an electron-phonon coupling factor, and γ_i & $\omega_{\nu,i}$ are the renormalized phonon line width and frequency. Note that a typographical error in Ref. 20 omitted the square in the denominator of Eq. (1) and that we have slightly rearranged the original equation as a matter of convenience when performing the fits. In addition to the caveats and assumptions of the original approach we also assume that the phonons couple *solely* to the Raman-active electronic continuum.

As a simple model of the *c*-axis electronic response in Y124, we use a form which arises from electronic Raman scattering in a dirty metal[14–16]

$$\chi(\omega) = \frac{\Gamma}{\Gamma - i\omega}, \quad (2)$$

where ω is the Raman shift and Γ is a frequency independent parameter which determines the position of the maximum in $\chi(\omega)$. In the original model, Γ is associated with a scattering rate arising from impurity scattering. We will demonstrate that due to the presence of the pseudogap in this material, equating Γ with a physical scattering rate is problematic.

A fit to the *c*-axis Raman spectrum at 100 K is shown in Fig. 1 (dashed line) and the agreement is exceedingly good. The inset to Fig. 1 shows electronic Raman spectra, obtained by subtracting the phonon contribution calculated from fits to the measured spectra, and the background fit at 100 K from Eq. (2) (dashed line). Interference between the phonons and the electronic continuum distort this simple relaxational response in the raw spectra. A suppression of intensity with decreasing temperature, extending to slightly above 900 cm^{-1}, is clearly and unambiguously seen in the electronic Raman spectra. The temperature dependences of the phonon modes can not account for the observed depletion;[21] details of the phonon fit results will be published separately.[22] Attempts to improve the model, by accommodation of the second-order phonon features and the inclusion of a nonin-

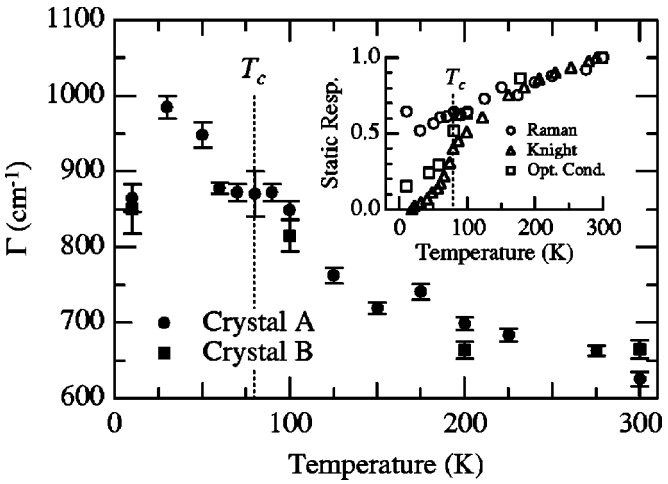

FIG. 2. The Γ parameter associated with the maximum of the *c*-axis electronic continuum, from Eq. (2). Inset: the normalized static response from Raman (open circles), Knight shift (open triangles), and optical conductivity (open squares) measurements. See text for details.

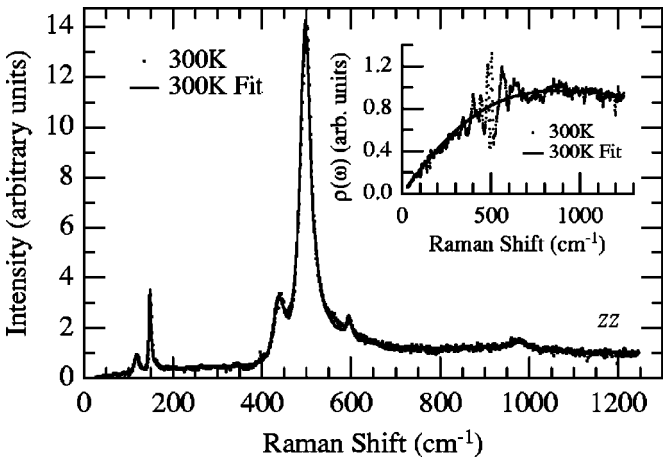

FIG. 3. The *c*-axis polarized Raman spectrum of Y123 at room temperature, with example fit comprising the five phonon peaks and the two-phonon feature. Here, $\Gamma \approx 900\ \mathrm{cm}^{-1}$. Inset: electronic Raman spectrum as in Fig. 1.

teracting background, had the predominant effect of increasing the fit uncertainty. As the qualitative temperature dependence of the fit parameters was unchanged, we persisted with the simpler expression of Eq. (1).

Figure 2 shows the temperature dependence of Γ for two crystals studied, and the excellent agreement between samples. According to Eq. (2) an increase in Γ shifts the continuum maximum to higher frequency and reduces the low-frequency intensity. Therefore, the gradual increase in Γ seen in Fig. 2 is implied by the observed loss of scattering intensity from the low frequency Raman continuum. Note that below T_c no clear superconductivity induced renormalization is evident in either Figs. 1 or 2. Although it is tempting to associate Γ with a physical scattering rate arising from impurities,[14–16] it is apparent that Γ is strongly influenced by the observed spectral depletion and thus can not be directly related to a physical scattering rate. This is verified by the lack of a clear relationship between Γ and the results of *c*-axis dc resistivity measurements.[2,3]

In order to compare our results with those of other experimental techniques, we plot in the inset to Fig. 2 the ratio $\rho(\omega \rightarrow 0,T)/\rho(\omega \rightarrow 0,300)$, i.e., the normalized static response (open circles), which is expected to scale with the density of states at the Fermi surface. In the normal state, the temperature dependence of the Raman response is consistent with ^{65}Cu(2) Knight shift[5] and *c*-axis optical conductivity[6] results, normalized at 300 K and plotted in Fig. 2 (open triangles and open squares). All three quantities exhibit a clear and gradual depletion[23] with decreasing temperature, which reveals the normal state pseudogap. This suggests no contribution from the CuO double chain conductivity to the *c*-axis Raman and optical responses, probably because the coherent charge excitation is located at very low frequencies. In passing, we remark that our spectra differ from the results of theoretical calculations of the *c*-axis Raman continuum using the plane-chain coupling model.[24]

Superconductivity induced changes in the *c*-axis continuum might be expected below T_c, as seen in the Knight shift and optical conductivity results[5,6] plotted in Fig. 2 and from *ab*-plane Raman measurements.[7,19] As Figs. 1 and 2 show, however, the superconducting state spectra are still well described by the simple relaxational response of Eq. (2) and the monotonic depletion of spectral weight is unaffected. Our result is consistent with *c*-axis polarized measurements of Y123, which show no dramatic continuum redistribution in the superconducting state.[25–27] This might be indicative of screening effects[27] or of incoherent charge transport along the *c*-axis which is unable to participate in any coherent Raman response, including the superconductivity induced renormalization.

We briefly mention one common feature between crystals: at 10 K the static response is significantly higher, and Γ is consequently significantly lower, than that at other temperatures below T_c. It seems that a weak change develops rapidly at low temperatures and overlaps with the pseudogap feature, suggestive of a continuum renormalization. The relation between this return of spectral weight at low temperatures and superconductivity is an open question.

Finally, we consider the implications of our simple model with respect to the origin of the Y124 *c*-axis electronic Raman continuum. Equation (2) describes the continuum as a relaxational response with a single frequency-independent parameter due, originally, to impurity scattering. Itai[15] has calculated the Raman spectrum for a coupled electron-phonon system where both electron-impurity and electron-phonon scattering processes are considered. The addition of electron-phonon scattering to impurity scattering effectively introduces a frequency dependence to Γ which 'creases' the electronic continuum near the phonon positions.[15] In the case of phonon scattering alone, the continuum displays a threshold at the scattering phonon energy and a frequency dependence which is superficially similar to the simple relaxational case.

With reference to Fig. 1 we see that the Y124 spectra are well described by a simple relaxational response, showing neither a scattering threshold nor distortions of the con-

tinuum near the phonon positions which are the signatures of phonon scattering processes. Therefore we conclude that phonon scattering plays no significant role in the origin of the *c*-axis continuum.

This result contrasts sharply with previous analyses of the *c*-axis Raman spectrum in Y123.[11–13] To resolve this difference we applied our model to *c*-axis Y123 spectra[28] from an underdoped single crystal of $T_c \approx 80$ K at various temperatures. An example fit at 300 K is shown in Fig. 3. Notably, our precursory analysis of the Y123 electronic continuum revealed a similar temperature dependence to that seen in Y124: a depletion of spectral weight from the continuum with decreasing temperature, unaffected by the onset of superconductivity and reversing at low temperatures.[28] This similarity between chain disordered Y123 and chain stoichiometric Y124 provides further evidence that the chains play a subordinate role in *c*-axis Raman scattering.

In conclusion, the *c*-axis electronic Raman continuum in Y124 can be accurately modelled as a relaxational response with a single frequency-independent parameter; phonon scattering processes do not contribute significantly to the observed continuum. As the temperature is decreased from 300 K we find that below a Raman shift of around 900 cm^{-1} there is a gradual depletion of spectral weight which is consistent with the evidence of the pseudogap in Y124 from optical conductivity and Knight shift measurements. No renormalization of the continuum is observed at T_c although a return of spectral weight is observed at low temperatures. We also find that the same model can be applied to underdoped Y123 and observe a similar continuum dependence on temperature.[28] There seems to be no contribution to the *c*-axis Raman continuum from the CuO chains, which dominate the metallic *c*-axis dc transport properties.[2,3]

We thank M. F. Limonov for stimulating discussions. This work was supported by the New Energy and Industrial Technology Development Organization (NEDO) as collaborative research and development of fundamental technologies for superconductivity applications.

[1] For example, see J. R. Cooper and J. W. Loram, J. Phys. I **6**, 2237 (1996).
[2] N. E. Hussey, K. Nozawa, H. Takagi, S. Adachi, and K. Tanabe, Phys. Rev. B **56**, R11 423 (1997).
[3] B. Bucher, J. Malar, J. Karpinski, and P. Wachter, Solid State Commun. **114**, 633 (2000).
[4] I. Tomeno, T. Machi, K. Tai, N. Koshizuka, S. Kambe, A. Hayashi, Y. Ueda, and H. Yasuoka, Phys. Rev. B **49**, 15 327 (1994).
[5] M. Bankay, M. Mali, J. Roos, and D. Brinkmann, Phys. Rev. B **50**, 6416 (1994).
[6] D. N. Basov, T. Timusk, B. Dabrowski, and J. D. Jorgensen, Phys. Rev. B **50**, R3511 (1994); D. N. Basov, R. Liang, B. Dabrowski, D. A. Bonn, W. N. Hardy, and T. Timusk, Phys. Rev. Lett. **77**, 4090 (1996).
[7] J.-Y. Genoud, H. J. Trodahl, and A. E. Pantoja, Solid State Commun. **113**, 285 (1999).
[8] J. Bäckström, M. Rübhausen, M. Käll, L. Börjesson, A. P. Litvinchuk, M. Kakihana, M. Osada, and B. Dabrowski, Phys. Rev. B **61**, 7049 (2000).
[9] D. Reznik, M. V. Klein, W. C. Lee, D. M. Ginsberg, and S-W. Cheong, Phys. Rev. B **46**, 11 725 (1992).
[10] S. L. Cooper, P. Nyhus, D. Reznik, M. V. Klein, W. C. Lee, D. M. Ginsberg, B. W. Veal, A. P. Paulikas, and B. Dabrowski, Phys. Rev. Lett. **70**, 1533 (1993).
[11] P. Nyhus, M. A. Karlow, S. L. Cooper, B. W. Veal, and A. P. Paulikas, Phys. Rev. B **50**, 13 898 (1994).
[12] S. L. Cooper and K. E. Gray, in *Physical Properties of High Temperature Superconductors IV*, edited by Donald M. Ginsberg (World Scientific, Singapore, 1994), p. 61.
[13] S. L. Cooper, M. A. Karlow, P. Nyhus, R. L. Neiman, J. Giapintzakis, D. M. Ginsberg, B. W. Veal, and A. P. Paulikas, in *Advances in Superconductivity VIII*, edited by H. Hayakawa and Y. Enamoto (Springer-Verlag, Tokyo, 1996), p. 133.
[14] A. Zawadowski and M. Cardona, Phys. Rev. B **42**, 10 732 (1990).
[15] K. Itai, Phys. Rev. B **45**, 707 (1992).
[16] D. Einzel and R. Hackl, J. Raman Spectrosc. **27**, 307 (1996).
[17] N. E. Hussey, H. Takagi, Y. Iye, S. Tajima, A. I. Rykov, and K. Yoshida, Phys. Rev. B **61**, R6475 (2000).
[18] S. Adachi, K. Nakanishi, K. Tanabe, K. Nozawa, H. Takagi, W-Z. Hu, and M. Izumi, Physica C **301**, 123 (1998).
[19] S. Donovan, J. Kircher, J. Karpinski, E. Kaldis, and M. Cardona, J. Supercond. **8**, 417 (1995).
[20] X. K. Chen, E. Altendorf, J. C. Irwin, R. Liang, and W. N. Hardy, Phys. Rev. B **48**, 10 530 (1993).
[21] For example, between 300 and 30 K the integrated spectral area of the continuum from 30 to 1200 cm^{-1} gradually falls from 1070 to 810 square units, while the total spectral area of the phonon modes remains constant at 500 ± 85 square units. This confirms that the phonons are not involved in the loss of spectral weight from the electronic continuum.
[22] J. W. Quilty, S. Tajima, S. Adachi, and A. Yamanaka, Physica C (to be published).
[23] The depletion of the Raman continuum intensity slightly accelerates below around 200 K, comparable with the ''characteristic'' pseudogap temperature seen by other techniques.
[24] W. C. Wu and J. P. Carbotte, Phys. Rev. B **56**, 6327 (1997).
[25] K. F. McCarty, J. Z. Liu, R. N. Shelton, and H. B. Radousky, Phys. Rev. B **42**, 9973 (1990).
[26] D. Kirillov, C. B. Eom, and T. H. Geballe, Phys. Rev. B **43**, 3752 (1991).
[27] D. Braithwaite, J. Q. Liu, G. Martinez, P. J. M. Van Bentum, and P. Lejay, Physica C **177**, 213 (1991).
[28] J. W. Quilty, M. F. Limonov, S. Tajima, and A. Yamanaka (unpublished).